

GaN-on-GaN p-i-n diodes with avalanche capability enabled by eliminating surface leakage with hydrogen plasma treatment

Cite as: Appl. Phys. Lett. **121**, 092103 (2022); <https://doi.org/10.1063/5.0107677>

Submitted: 06 July 2022 • Accepted: 06 August 2022 • Published Online: 30 August 2022

 Kai Fu,  Ziyi He,  Chen Yang, et al.



View Online



Export Citation



CrossMark

ARTICLES YOU MAY BE INTERESTED IN

[In situ tunable giant electrical anisotropy in a grating gated AlGaIn/GaN two-dimensional electron gas](#)

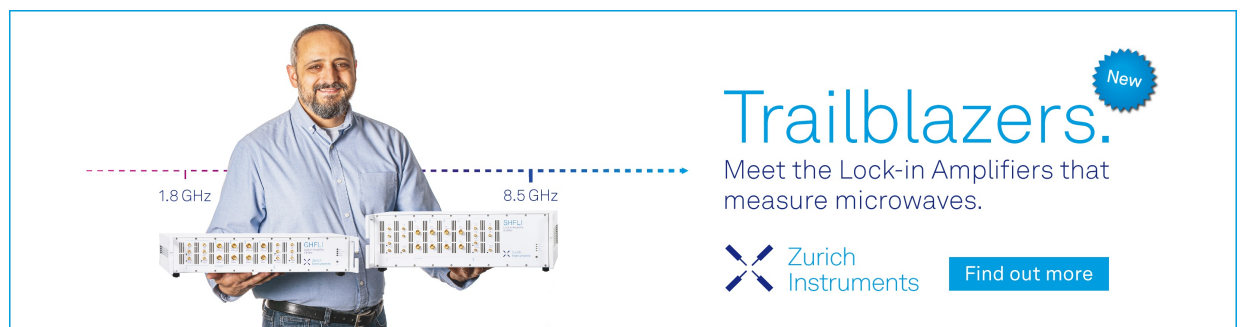
Applied Physics Letters **121**, 092101 (2022); <https://doi.org/10.1063/5.0097518>


[Investigation of proton irradiation induced \$E_C-0.9\$ eV traps in AlGaIn/GaN high electron mobility transistors](#)

Applied Physics Letters **121**, 092102 (2022); <https://doi.org/10.1063/5.0103302>


[Properties and device performance of BN thin films grown on GaN by pulsed laser deposition](#)

Applied Physics Letters **121**, 092105 (2022); <https://doi.org/10.1063/5.0092356>



Trailblazers. 

Meet the Lock-in Amplifiers that measure microwaves.

 Zurich Instruments [Find out more](#)

GaN-on-GaN p-i-n diodes with avalanche capability enabled by eliminating surface leakage with hydrogen plasma treatment

Cite as: Appl. Phys. Lett. **121**, 092103 (2022); doi: 10.1063/5.0107677

Submitted: 6 July 2022 · Accepted: 6 August 2022 ·

Published Online: 30 August 2022



View Online



Export Citation



CrossMark

Kai Fu,¹ Ziyi He,² Chen Yang,² Jingan Zhou,¹ Houqiang Fu,^{2,3,a)} and Yuji Zhao^{1,a)}

AFFILIATIONS

¹Department of Electrical and Computer Engineering, Rice University, Houston, Texas 77005, USA

²School of Electrical, Computer and Energy Engineering, Arizona State University, Tempe, Arizona 85287, USA

³Department of Electrical and Computer Engineering, Iowa State University, Ames, Iowa 50011, USA

^{a)}Authors to whom correspondence should be addressed: houqiang@asu.edu and Yuji.Zhao@rice.edu

ABSTRACT

Traditional mesa terminations require precise angle design to reduce the electric field at the edge and surface treatment to reduce etch damage. Otherwise, the device usually suffers a premature breakdown. This work proposes the use of easy-to-implement hydrogen plasma treatment to solve the premature breakdown caused by mesa and demonstrates the avalanche capability in GaN-on-GaN p-i-n diodes. The breakdown electric field when the avalanche occurred was ~ 2.3 MV/cm at room temperature for a GaN drift layer with a doping concentration of $\sim 7 \times 10^{15} \text{ cm}^{-3}$, which is consistent with the theoretical value. The temperature coefficient of the avalanche breakdown voltage of the devices was $4.64\text{--}4.85 \times 10^{-4} \text{ K}^{-1}$. This work shows a simple and effective approach to achieve avalanche capability in vertical GaN power devices, which can serve as an important reference for the future development of efficient and robust GaN power electronics.

Published under an exclusive license by AIP Publishing. <https://doi.org/10.1063/5.0107677>

Due to its excellent material properties such as high bandgap, large critical electric field, high mobility, and large Baliga's figure of merit, gallium nitride (GaN) has become one of the most promising candidates in power electronics. GaN power devices are capable of operating at high switching frequencies and high breakdown voltages, thereby drastically improving the energy conversion efficiency, reducing the volume of energy storage components, and scaling down the form factor of power systems.^{1–3} As GaN devices are increasingly maturing for commercialization, more and more attention has been paid to the reliability of GaN power devices.^{4–8} Avalanche capability is a critical metric for a robust power device due to its nature of nondestructive avalanche breakdown and the need for safety protection of power systems. It has been shown that proper engineering of electric field distribution in devices is the key to achieve avalanche breakdown.^{9–12} One of the commonly used methods for device electric field engineering is edge termination (ET), including ion implantation,^{13–18} field plate,^{9,10} beveled mesa,¹⁹ and deeply vertical mesa.^{20,21}

Mesa isolation has been one of the most commonly used edge terminations due to its ease of implementation. However, reaching avalanche capability by mesa isolation demands precise dimensional or angular designs and high requirements for the fabrication

process,^{11,12,20,22} such as beveled mesa¹⁹ and deeply vertical mesa.^{20,21} Additional design may also be required, such as the field plate.^{9,10} Moreover, mesa etching may cause surface damage and surface leakage pathway,²³ resulting in a premature breakdown. Meanwhile, hydrogen plasma based ET is another easy-to-implement solution by using hydrogen plasma treatment to convert p-GaN to the high resistive GaN.^{24–26} In this study, the hydrogen plasma treatment has been applied to the conventional mesa isolation to eliminate the surface leakage and avoid premature breakdown, which helps to realize GaN-on-GaN p-i-n diodes with avalanche capability. The proposed approach can not only help to simplify the fabrication process but also achieve high-performance GaN p-i-n diodes.

Vertical GaN p-i-n diodes were grown by metalorganic chemical vapor deposition (MOCVD) on *c*-plane GaN bulk substrates. The device structure consisted of a 20-nm-thick p⁺-GaN layer, a 500-nm-thick p-GaN layer, a 2.2- μm -thick drift layer, and a 500-nm-thick n⁺-GaN buffer layer. Figure 1(a) shows the vertical p-i-n diodes with conventional mesa edge termination (Mesa-ET), which is used as a reference. The hydrogen plasma treatment was applied to the same device on the same sample to form the combined ET (MHP-ET) consisting of the Mesa-ET and hydrogen plasma treatment, as shown in

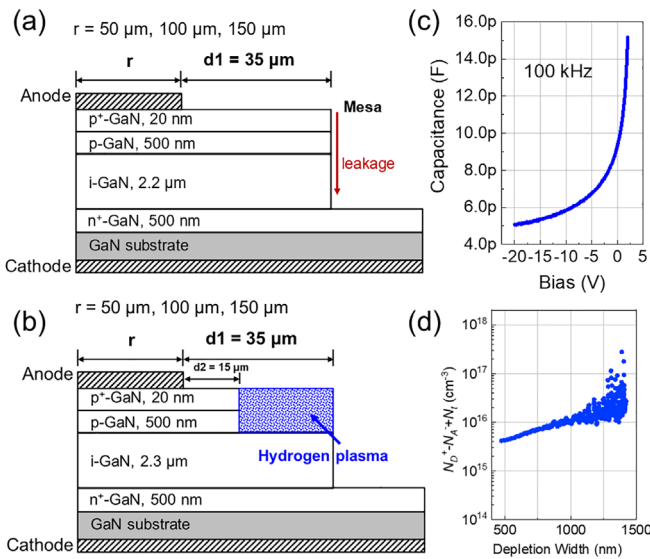


FIG. 1. Schematics of vertical GaN p-i-n diodes with (a) Mesa-ET and (b) MHP-ET. (c) C–V curve of the sample. (d) Doping profile extracted from the C–V curve.

Fig. 1(b). The hydrogen plasma was produced by an inductively coupled plasma (ICP) tool with an RF power of 5 W. The plasma treatment has been found not very sensitive to the processing time,^{24,27} indicating a large processing window. The samples were annealed at 400 °C for 5 min at N₂ ambient after the plasma treatment. The diameter of the p-GaN Ohmic contact ranged from 100 to 300 μm. The distance between the edge of the p-GaN Ohmic contact and the edge of the mesa was kept at 35 μm. The treatment region was 15 μm away from the edge of the p-GaN Ohmic contact. Figure 1(c) shows the capacitance–voltage (C–V) curve of the sample, and Fig. 1(d) shows the doping profile in the drift layer extracted from the C–V curve.²⁸ The average doping concentration of the GaN drift layer was $\sim 7 \times 10^{15} \text{ cm}^{-3}$.

Figures 2(a) and 2(b) show the forward current–voltage (*I*–*V*) curves of the Mesa-ET and MHP-ET devices. The magnitude of the current density of the MHP-ET device is slightly higher than the Mesa-ET device. The turn-on voltages of the device with the Mesa-ET and the MHP-ET are 3.1 and 3.4 V, respectively. The device with the MHP-ET is less sensitive to temperature change, thereby leading to a more stable ideality factor at different temperatures [Fig. 2(c)]. Figure 2(d) presents the on-resistance of the devices at relatively large forward biases (>6 V), showing different trends with the temperature. The forward current contains three components, i.e., the diffusion current, the Shockley–Read–Hall (SRH) recombination current, and the radiative recombination current.²⁹ Since an ideal p–n diode tends to have a small SRH recombination current and a low parasitic resistance (large diffusion current),²⁹ the MHP-ET device in this work is closer to the ideal with relatively low on-resistance and smaller ideality factors at different temperatures. Ideally, the forward characteristics of these two types of devices should be very close because these forward characteristic parameters mainly depend on the material properties, p-type Ohmic contact, and n-type Ohmic contact, and these parameters are the same for both devices. One possible reason

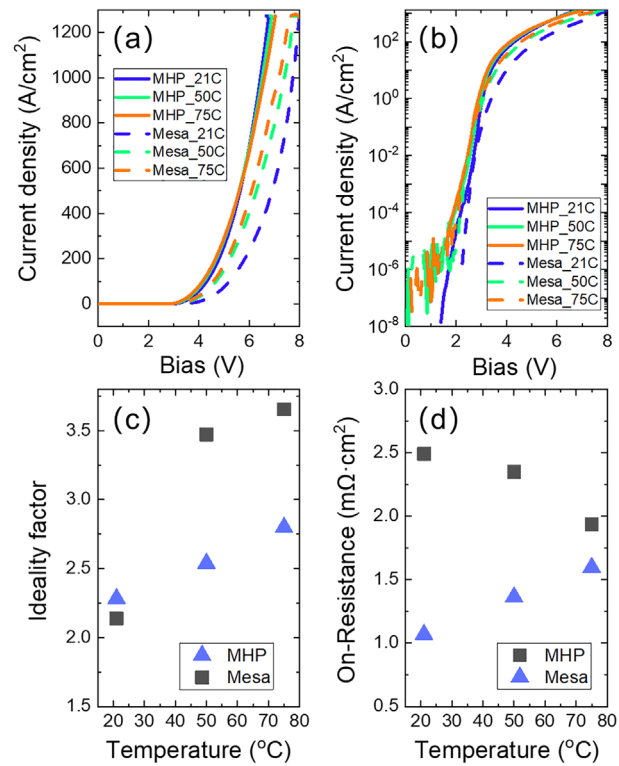


FIG. 2. Forward performance of the Mesa-ET and MHP-ET devices: (a) *I*–*V* curves in linear scale at different temperatures, (b) *I*–*V* curves in semi-log scale at different temperatures, (c) ideality factors at different temperatures, and (d) on-resistance at different temperature.

for the differences is that the annealing process during the formation of the MHP-ET affected the Ohmic contacts.

Figure 3(a) shows the reverse *I*–*V* curves of the vertical GaN p-i-n diodes with the Mesa-ET at different temperatures. The devices had breakdown voltages in the range of 375–450 V at room temperature. When the temperature was higher than 75 °C, the GaN p-i-n diodes with different sizes all showed smaller breakdown voltages and suffered from a destructive breakdown at device edges. The breakdown voltages of the devices with the Mesa-ET decreased with increasing temperature, which is because more electron–hole pairs were generated at higher temperatures, leading to the decrease in the required voltage for breakdown to occur.³⁰ As shown in Fig. 2(b), the vertical GaN p-i-n diodes with the MHP-ET showed relatively high breakdown voltages of 450–470 V at room temperature. All devices of different sizes exhibited non-destructive breakdown up to 125 °C. The breakdown voltages of the devices with the MHP-ET increased with increasing temperature, indicating an avalanche breakdown due to the impact ionization where higher voltages were needed at higher temperatures for charge carriers to gain sufficient kinetic energy for impact ionization since the mean free path of charge carriers is reduced at higher temperatures. Furthermore, the devices with different sizes showed similar breakdown voltages, indicating good uniformity and scalability of the MHP-ET.

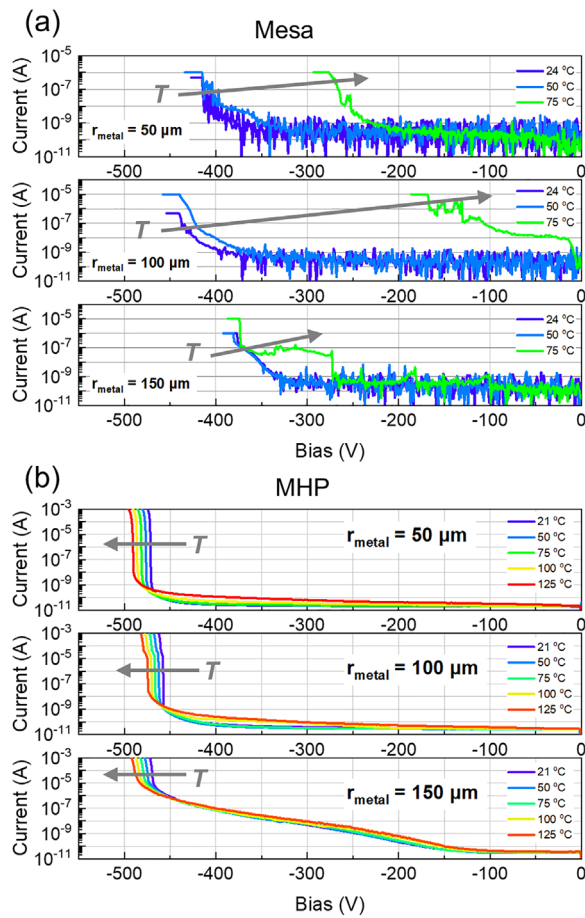


FIG. 3. Reverse I - V curves of the devices with different sizes at different temperatures with (a) Mesa-ET and (b) MHP-ET. Mesa-ET shows a negative temperature coefficient, while MHP-ET shows a positive temperature coefficient.

The electric field distributions in the Mesa-ET and MHP-ET devices are shown in Fig. 4. The results were simulated using the commercial TCAD software Silvaco.³¹ The HR-GaN, transferred from the p-GaN layer by the hydrogen plasma, was treated as undoped GaN ($6 \times 10^{15} \text{ cm}^{-3}$) in the simulation. The reported impact ionization coefficients²¹ were used to define the breakdown. As shown in Figs. 4(a)–4(c), compared with the electric field distribution in the device by Mesa-ET, the MHP-ET can effectively reduce the electric field at the mesa edge, i.e., shift it from the mesa edge with an etched surface to an inner position. As shown in Fig. 4(d), the GaN p-i-n diodes with either Mesa-ET or MHP-ET should have almost the same breakdown voltage in the ideal case. However, etching damage generally exists on the etched sidewall; especially in this work, we did not perform surface damage repair, such as wet etching. The etching damage can cause a surface leakage path at the high electric field,²³ leading to the premature breakdown of the devices.¹⁴ The results not only show that the premature breakdown with Mesa-ET comes from the surface leakage but also show that the hydrogen plasma can be used as an effective approach to eliminate the surface leakage.

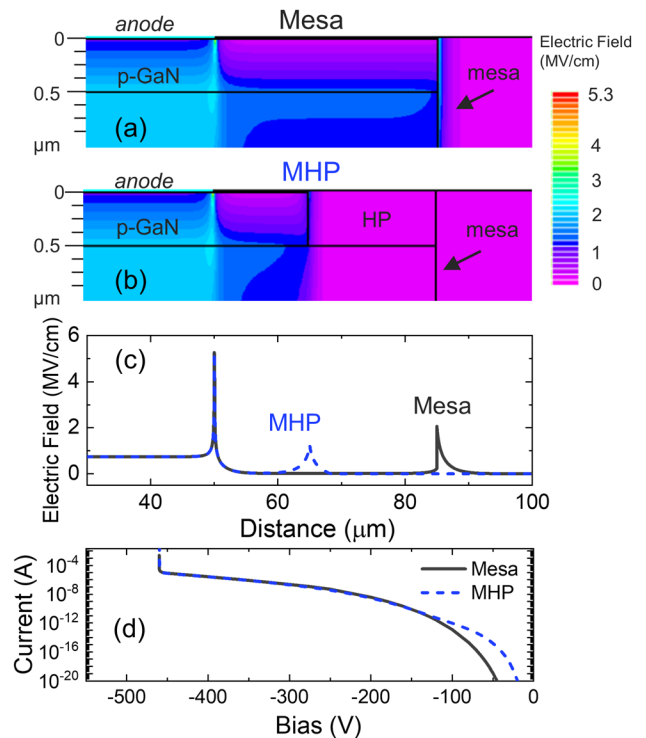


FIG. 4. Simulations of the electric field distribution in the devices with (a) Mesa-ET and (b) MHP-ET. (c) Electric field profiles at the device surface for the Mesa-ET and MHP-ET. (d) Simulations of the breakdown I - V curves for the Mesa-ET and MHP-ET.

Figure 5(a) presents the avalanche breakdown voltages at different temperatures and sizes for devices with the MHP-ET. The temperature coefficient of the avalanche breakdown voltage due to impact ionization was extracted to be 4.64 – $4.85 \times 10^{-4} \text{ K}^{-1}$. The breakdown electric field, E_b , when the avalanche occurred can be estimated by²⁴

$$V_{br} = E_b d - \frac{q N_D d^2}{2 \epsilon_0 \epsilon_{\text{GaN}}}, \quad (1)$$

where V_{br} is the breakdown voltage, d is the thickness of the drift layer, q is the electron charge, N_D is the doping concentration in the drift layer, ϵ_0 is the permittivity of the free space, and ϵ_{GaN} is the dielectric constant of GaN along c axis which is 10.4.^{32,33} The breakdown electric field was calculated to be $\sim 2.3 \text{ MV/cm}$ at room temperature, as shown in Fig. 5(b). Reported values^{10,14–16,19,20,34,35} of the breakdown electric field as a function of the doping level in GaN vertical p-i-n diodes with avalanche capability are plotted in Fig. 5(c). The fitting curve is plotted based on the reported impact ionization coefficients.²¹ The experimental data agree well with the theoretical curve.

In summary, vertical GaN-on-GaN p-i-n diodes with the Mesa-ET and MHP-ET were fabricated and measured. The devices with the conventional Mesa-ET broke down at 375–450 V and suffered from destructive breakdown, while the devices with the MHP-ET showed nondestructive avalanche breakdown at 450–470 V at room temperature. Device simulation indicates that the MHP-ET can effectively eliminate the surface leakage by reducing the electric field at

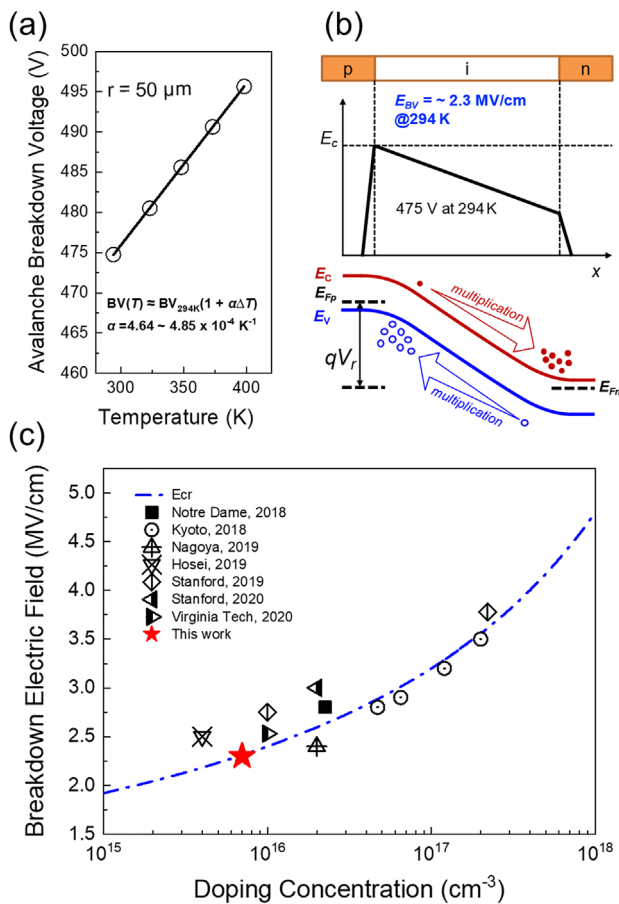


FIG. 5. (a) Avalanche breakdown voltages of the devices with MHP-ET as a function of temperature. (b) Schematics of electric field and energy band structure in the device under reverse bias. (c) Reported data^{10,14–16,19,20,34,35} of breakdown electric field as a function of doping concentration in GaN vertical p-i-n diodes with avalanche capability.

the mesa edge, thereby avoiding a premature breakdown. This work provides an easy-to-implement ET to achieve avalanche capability in vertical GaN power devices, which can serve as a reference for the future development of efficient and robust GaN power electronics.

This work was supported in part by the ARPA-E PNDIODES Program under Grant No. DE-AR0000868, in part by the NASA HOTTech Program under Grant No. 80NSSC17K0768, in part by the Rice's Technology Development Fund, in part by the ASU Nanofab through NSF under Contract No. ECCS-1542160, and in part by the ULTRA, an Energy Frontier Research Center funded by the U.S. Department of Energy, Office of Science, Basic Energy Sciences under Award No. DE-SC0021230.

AUTHOR DECLARATIONS

Conflict of Interest

The authors have no conflicts to disclose.

Author Contributions

Kai Fu and Ziyi He contributed equally to this work.

Kai Fu: Conceptualization (equal); Data curation (equal); Formal analysis (equal); Writing – original draft (equal); Writing – review & editing (equal). **Ziyi He:** Formal analysis (equal); Software (equal). **Chen Yang:** Data curation (supporting); Investigation (supporting). **Jingan Zhou:** Formal analysis (supporting); Investigation (supporting). **Houqiang Fu:** Conceptualization (equal); Writing – review & editing (equal). **Yuji Zhao:** Supervision (equal); Writing – review & editing (equal).

DATA AVAILABILITY

The data that support the findings of this study are available from the corresponding authors upon reasonable request.

REFERENCES

- U. K. Mishra, L. Shen, T. E. Kazior, and Y. Wu, *Proc. IEEE* **96**, 287 (2008).
- B. J. Baliga, *Semicond. Sci. Technol.* **28**, 074011 (2013).
- E. A. Jones, F. F. Wang, and D. Costinett, *IEEE J. Emerging Sel. Top. Power Electron.* **4**, 707 (2016).
- M. Meneghini, O. Hilt, J. Wuerfl, and G. Meneghesso, *Energies* **10**, 153 (2017).
- M. Meneghini, I. Rossetto, C. D. Santi, F. Rampazzo, A. Tajalli, A. Barbato, M. Ruzzarin, M. Borga, E. Canato, E. Zanoni, and G. Meneghesso, in *2017 IEEE International Reliability Physics Symposium (IRPS)* (IEEE, 2017), p. 3B.
- J. A. del Alamo and E. S. Lee, *IEEE Trans. Electron Devices* **66**, 4578 (2019).
- B. Shankar, A. Soni, H. Chandrasekar, S. Raghavan, and M. Shrivastava, *IEEE Trans. Electron Devices* **66**, 3433 (2019).
- P. J. Martínez, S. Letz, E. Maset, and D. Zhao, *Semicond. Sci. Technol.* **35**, 035007 (2020).
- K. Nomoto, Z. Hu, B. Song, M. Zhu, M. Qi, R. Yan, V. Protasenko, E. Imhoff, J. Kuo, N. Kaneda, T. Mishima, T. Nakamura, D. Jena, and H. G. Xing, in *2015 IEEE International Electron Devices Meeting (IEDM)* (IEEE, 2015), p. 9.7.1.
- H. Ohta, N. Asai, F. Horikiri, Y. Narita, T. Yoshida, and T. Mishima, *Jpn. J. Appl. Phys.* **58**, SCCD03 (2019).
- J. R. Dickerson, A. A. Allerman, B. N. Bryant, A. J. Fischer, M. P. King, M. W. Moseley, A. M. Armstrong, R. J. Kaplar, I. C. Kizilyalli, O. Aktas, and J. J. Wierer, *IEEE Trans. Electron Devices* **63**, 419 (2016).
- K. Zeng and S. Chowdhury, *IEEE Trans. Electron Devices* **67**, 2457 (2020).
- I. C. Kizilyalli, A. P. Edwards, H. Nie, D. Disney, and D. Bour, *IEEE Trans. Electron Devices* **60**, 3067 (2013).
- L. Cao, J. Wang, G. Harden, H. Ye, R. Stillwell, A. J. Hoffman, and P. Fay, *Appl. Phys. Lett.* **112**, 262103 (2018).
- D. Ji, B. Ercan, and S. Chowdhury, *Appl. Phys. Lett.* **115**, 073503 (2019).
- J. Liu, M. Xiao, R. Zhang, S. Pidaparathi, C. Drowley, L. Baubutr, A. Edwards, H. Cui, C. Coles, and Y. Zhang, *IEEE Electron Device Lett.* **41**, 1328 (2020).
- M. Matys, T. Ishida, K. P. Nam, H. Sakurai, K. Kataoka, T. Narita, T. Uesugi, M. Bockowski, T. Nishimura, J. Suda, and T. Kachi, *Appl. Phys. Express* **14**, 074002 (2021).
- M. Matys, T. Ishida, K. P. Nam, H. Sakurai, T. Narita, T. Uesugi, M. Bockowski, J. Suda, and T. Kachi, *Appl. Phys. Lett.* **118**, 093502 (2021).
- T. Maeda, T. Narita, H. Ueda, M. Kanechika, T. Uesugi, T. Kachi, T. Kimoto, M. Horita, and J. Suda, in *2018 IEEE International Electron Devices Meeting (IEDM)* (IEEE, 2018), p. 30.1.1.
- H. Fukushima, S. Usami, M. Ogura, Y. Ando, A. Tanaka, M. Deki, M. Kushimoto, S. Nitta, Y. Honda, and H. Amano, *Jpn. J. Appl. Phys.* **58**, SCCD25 (2019).
- T. Maeda, T. Narita, S. Yamada, T. Kachi, T. Kimoto, M. Horita, and J. Suda, in *2019 IEEE International Electron Devices Meeting (IEDM)* (IEEE, 2019), p. 4.2.1.
- M. Shurrab and S. Singh, *Semicond. Sci. Technol.* **35**, 065005 (2020).
- Y. Zhang, M. Sun, H. Y. Wong, Y. Lin, P. Srivastava, C. Hatem, M. Azize, D. Piedra, L. Yu, T. Sumitomo, N. A. de Braga, R. V. Mickevicius, and T. Palacios, *IEEE Trans. Electron Devices* **62**, 2155 (2015).

- ²⁴H. Fu, K. Fu, X. Huang, H. Chen, I. Baranowski, T. Yang, J. Montes, and Y. Zhao, *IEEE Electron Device Lett.* **39**, 1018 (2018).
- ²⁵H. Fu, K. Fu, H. Liu, S. R. Alugubelli, X. Huang, H. Chen, J. Montes, T. H. Yang, C. Yang, J. Zhou, F. A. Ponce, and Y. Zhao, *Appl. Phys. Express* **12**, 051015 (2019).
- ²⁶H. Fu, K. Fu, S. R. Alugubelli, C. Cheng, X. Huang, H. Chen, T. Yang, C. Yang, J. Zhou, J. Montes, X. Deng, X. Qi, S. M. Goodnick, F. A. Ponce, and Y. Zhao, *IEEE Electron Device Lett.* **41**, 127 (2020).
- ²⁷R. Hao, N. Xu, G. Yu, L. Song, F. Chen, J. Zhao, X. Deng, X. Li, K. Cheng, K. Fu, Y. Cai, X. Zhang, and B. Zhang, *IEEE Trans. Electron Devices* **65**, 1314 (2018).
- ²⁸K. Fu, H. Fu, H. Liu, S. R. Alugubelli, T. H. Yang, X. Huang, H. Chen, I. Baranowski, J. Montes, F. A. Ponce, and Y. Zhao, *Appl. Phys. Lett.* **113**, 233502 (2018).
- ²⁹Z. Hu, K. Nomoto, B. Song, M. Zhu, M. Qi, M. Pan, X. Gao, V. Protasenko, D. Jena, and H. G. Xing, *Appl. Phys. Lett.* **107**, 243501 (2015).
- ³⁰S. M. Sze and K. K. Ng, *Physics of Semiconductor Devices*, 3rd ed. (John Wiley & Sons, Inc., 2007).
- ³¹C. Yang, H. Fu, K. Fu, T.-H. Yang, J. Zhou, J. Montes, and Y. Zhao, *Semicond. Sci. Technol.* **36**, 075009 (2021).
- ³²A. S. Barker and M. Ilegems, *Phys. Rev. B* **7**, 743 (1973).
- ³³J. Y. Tsao, S. Chowdhury, M. A. Hollis, D. Jena, N. M. Johnson, K. A. Jones, R. J. Kaplar, S. Rajan, C. G. Van de Walle, E. Bellotti, C. L. Chua, R. Collazo, M. E. Coltrin, J. A. Cooper, K. R. Evans, S. Graham, T. A. Grotjohn, E. R. Heller, M. Higashiwaki, M. S. Islam, P. W. Juodawlkis, M. A. Khan, A. D. Koehler, J. H. Leach, U. K. Mishra, R. J. Nemanich, R. C. N. Pilawa-Podgurski, J. B. Shealy, Z. Sitar, M. J. Tadjer, A. F. Witulski, M. Wraback, and J. A. Simmons, *Adv. Electron. Mater.* **4**, 1600501 (2018).
- ³⁴K. Nomoto, B. Song, Z. Hu, M. Zhu, M. Qi, N. Kaneda, T. Mishima, T. Nakamura, D. Jena, and H. G. Xing, *IEEE Electron Device Lett.* **37**, 161 (2016).
- ³⁵D. Ji, B. Ercan, G. Benson, A. K. M. Newaz, and S. Chowdhury, *Appl. Phys. Lett.* **116**, 211102 (2020).